Electronic properties of disordered corner-sharing tetrahedral lattices

F. Fazileh,* X. Chen, R. J. Gooding, and K. Tabunshchyk†
Department of Physics, Queen's University, Kingston, Ontario K7L 3N6 Canada
(Received 4 October 2005; revised manuscript received 8 December 2005; published 26 January 2006)

We have examined the behavior of noninteracting electrons moving on a corner-sharing tetrahedral lattice into which we introduce a uniform (box) distribution, of width W, of random on-site energies. We have used both the relative localization length and the spectral rigidity to analyze the nature of the eigenstates and have determined both the mobility-edge trajectories as a function of W and the critical disorder W_c, beyond which all states are localized. We find (i) that the mobility-edge trajectories (energies E_c versus disorder W) are qualitatively different from those found for a simple cubic lattice and (ii) that the spectral rigidity is scale invariant at W_c and thus provides a reliable method of estimating this quantity—we find $W_c/t=14.5$. We then discuss our results in the context of the metal-to-insulator transition undergone by $LiAl_yTi_{2-y}O_4$ in a quantum-site percolation model that also includes the above-mentioned Anderson disorder. We show that the effects of an inhomogeneous distribution of on-site energies produced by the Al impurity potentials are small compared to those produced by quantum-site percolation, at least in the determination of the doping concentration at which the metal-to-insulator transition is predicted to occur.

DOI: 10.1103/PhysRevB.73.035124 PACS number(s): 71.30.+h, 71.23.−k, 72.80.Ga

I. INTRODUCTION

The properties of the corner-sharing tetrahedral lattice (CSTL) are of interest in a wide variety of physical systems.[1] This lattice is a nonbipartite, and thus frustrated, three-dimensional structure that is the conducting path of electrons in many interesting systems. This network can be derived, e.g., from the diamond structure (which is a bipartite lattice) by placing a site at each bond midpoint.[2] One interesting consequence from this construction is that, e.g., the critical (classical) site percolation threshold of pyrochlore is the same as the bond percolation threshold of diamond. Also, this structure is a sublattice of many compounds, including pyrochlores and spinels. In the $A_2B_2O_7$ pyrochlore structure, both the A and B sublattices can be realized as a network of corner-sharing tetrahedra, which is nowadays often referred to as the pyrochlore lattice. Examples of the interesting (quantum) magnetic properties and superconducting behavior of several pyrochlores are discussed in the literature.[3,4] Indeed, there exist many experimental results which seem to suggest that the geometrical frustration of the CSTL in these compounds is responsible for their peculiar properties, and it has been argued that geometrical frustration tends to amplify the correlation and quantum effects.[1]

The initial motivation for our work has to do with the electronic properties of the normal spinel AB_2O_4,[5] in which the B sublattice forms a corner-sharing tetrahedral network. There are a large number of well-known spinels, some with exotic magnetic[2] and electronic properties.[6] Further, the recent discovery[7] of the first d-electron heavy-fermion compound LiV_2O_4 has generated substantial interest in such electronic systems, which has subsequently directed us to a study[10,11] of the simpler but as-yet not understood properties of $LiTi_2O_4$,[8] the latter of which has been suggested to be related to the high-T_c superconductors owing to strong electronic correlations.[9]

$LiTi_2O_4$ undergoes a metal-to-insulator transition when excess Li is doped onto the Ti (corner-sharing tetrahedral) sublattice or when Al (or Cr, which is not discussed in this paper) is substituted for Ti on the same sublattice, and due to the large difference in on-site energies (e.g., doped Li versus Ti), this system is well approximated by a quantum-site percolation model in which the removed sites are those Ti sites onto which either an excess Li or substituting Al ion are added. Recently, two of the present authors and Johnston[10] have examined the possibility that such a model accounts for the metal-to-insulator transition and found that physics beyond that contained in a quantum-site percolation model will be required. One example candidate for this "extra physics" can be understood as follows: the excess Li or substitutional Al impurity ions will generate a distribution of on-site energies around them due to their impurity potentials, so that in addition to their presence eliminating those sites from the conducting path, their effect on the neighboring sites should also be included. As suggested by Anderson,[2] the role played by such physics is approximated by a random set of on-site energies. Here we focus on one simple variant of such random energies—viz., that given by a uniform (box) distribution—and at the end of this paper we discuss the effect of such randomness on this metal-to-insulator transition.

We stress, however, that in any systematic study of the physics involving itinerant electrons encountered on a disordered CSTL could require the information contained in our paper. For example, in addition to our own work,[11,12] there are now several papers by Fujimoto[13–16] and others[17,18] on the physics of correlated electrons on this lattice, and if such work is extended to disordered systems, possessing an understanding of the disordered but uncorrelated electrons would be beneficial.

Our paper is organized as follows. In Sec. II we present the model that we study, and in Sec. III we state the numerical procedures that we use and the statistical quantities that we evaluate. In Sec. IV we give our comprehensive numerical results for the mobility-edge trajectories and the critical disorder, and in Sec. V we present our results for the

quantum-site percolation model plus Anderson disorder that is meant to mimic the (noninteracting) model of the metal-to-insulator transition in $LiTi_2O_4$. Finally, in Sec. VI we state our conclusions.

II. MODEL

In an effort to better understand the physics of electrons moving on this structure, we calculate numerically the mobility-edge trajectories in the energy-disorder plane of a CSTL with a tight-binding Hamiltonian with a uniform (box) distribution model of disorder (described below). In these calculations only near-neighbor hoppings are included, system sizes up to 43 904 sites have been investigated, and periodic boundary conditions have been used. The CSTL under consideration is quite complicated: there are two formula units per primitive unit cell, the conventional unit cell is that of an fcc lattice, and each formula unit has two octahedral-site Ti atoms. That is, each conventional unit cell has 16 sites. For this reason the oft-used transfer matrix-method[19] is awkward to implement, and we have instead diagonalized the Hamiltonian matrix for a lattice with $L \times L \times L$ conventional unit cells.

The Hamiltonian for this system is given by

$$H = \sum_{i,\sigma} \varepsilon_i n_{i,\sigma} - t \sum_{\langle i,j \rangle,\sigma} (c^{\dagger}_{i,\sigma} c_{j,\sigma} + \text{H.c.}), \tag{1}$$

where i,j denote the sites of the lattice, $\langle i,j \rangle$ implies that i and j are near neighbors, and $c_{i,\sigma}$ ($n_{i,\sigma}$) is the destruction (number) operator for an electron at site i and spin σ. The hopping energy is t, and the on-site energy at site i is given by ε_i. For a uniform (box) distribution of disorder the on-site energies are being chosen at random to be in the range from $-W/2$ to $+W/2$, with all energies in this range having the same probability.

Our objective is to analyze this model and determine the energy ranges over which the eigenstates are localized and extended—the trajectory in (W, energy) space defines the mobility-edge trajectories. Further, when W is increased the upper and lower mobility edges will merge, thus identifying the critical disorder; this quantity is denoted by W_c (or, more precisely, W_c/t in dimensionless units), and we have determined this quantity using several different techniques.

It seems reasonable that one could be guided, in part, by the extensive studies of this transition for the $3d$ simple cubic lattice; however, there are some important differences that make this system considerably more difficult to work with. First, the energy spectrum of the simple cubic lattice is symmetric about zero energy, and since the upper and lower mobility edges merge at the transition indicated by W_c, one may examine an energy window around zero (see, e.g., Fig. 2 of Ref. 19 for an example density of states for such a problem). Further, since the mobility edge is remarkably flat in the immediate region of W_c, one can improve their statistics by looking at a reasonably large window of energy around zero (see, e.g., Fig. 1 of Ref. 20 and the discussion in Ref. 21). However, this is not the case for a CSTL—the spectrum is not symmetric about some middle energy (apart from the limit of infinite disorder, which is pathological and of no assistance in our numerics), and thus the search for the critical disorder (at which the mobility edges merge) is more problematic. As an example of this, note that in studies of the mobility-edge trajectories for quantum-site percolation models, the simple cubic lattice behaves somewhat similarly to the box distribution's result discussed above (see Ref. 22), whereas for the CSTL two of us and Johnston[10] found that the trajectory was not flat, instead depending strongly on disorder (which for a quantum-site percolation model is the fraction on unoccupied sites). Indeed, in the results presented below, we will show that (i) the mobility edges meet at an energy around $-4t$, whereas the middle of the band (for this W) is at an energy of $-0.5t$, and (ii) the mobility edges do depend on disorder quite strongly, and the upper and lower mobility edges are not obviously related to one another. In part for these reasons, the identification of the mobility-edge trajectories and W_c is somewhat more challenging for a CSTL.

III. NUMERICAL PROCEDURES

In order to distinguish between localized and extended eigenstates we have used several techniques. First, we have calculated the localization length of an eigenstate[23] in the form

$$\lambda = \sum_i \sum_j |\psi_i|^2 |\psi_j|^2 d(i,j), \tag{2}$$

where ψ_i is the probability amplitude for the eigenstate, of a given fixed energy, at site i and $d(i,j)$ is the Euclidean distance between lattice sites i and j. Then, this quantity is averaged for all energy eigenstates in a chosen energy range. The ratio of this parameter to the identically defined localization length of an eigenstate with constant amplitude over the entire lattice, the latter denoted by λ_0, is referred to as the relative localization length; the ratio is thus denoted by λ/λ_0. The behavior of this relative localization length as a function of increasing lattice size (for an specific energy range in the spectrum of the system) indicates whether these eigenstates, in the thermodynamic limit, will have localized or delocalized character. That is, if this parameter increases with system size (having a limiting ratio of 1), those states are extended, while if this quantity decreases with system size, those eigenstates are localized. This statistic was employed in the identification of the mobility-edges and metal-to-insulator transition in a quantum-site percolation model of a CSTL.[10,12]

The above-described statistics require the determination of the eigenvectors of the Hamiltonian, which is numerically more demanding than the determination of the eigenvalues alone. The most commonly employed statistic for analyzing the eigenvalues is so-called level statistics.[24,25] However, we have found[26] that the most sensitive indication of, in particular, W_c/t is the so-called Dyson-Mehta Δ_3 "spectral rigidity," which is described in detail in a variety of references—see, e.g., Refs. 27 and 28. Δ_3 is defined by

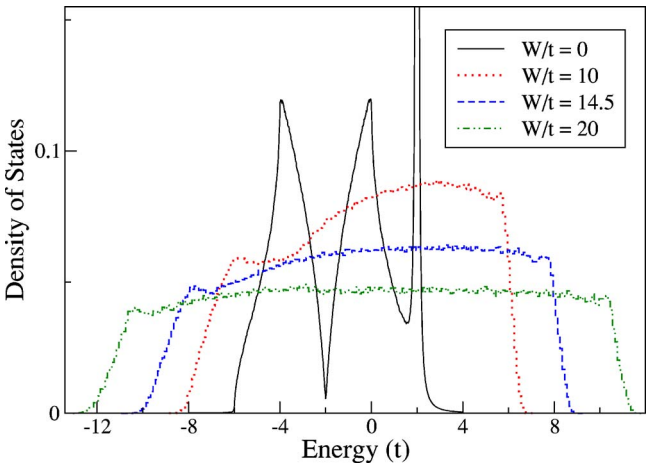

FIG. 1. (Color online) The density of states for a tight-binding Hamiltonian on a 21 296 site CSTL with periodic boundary conditions for near-neighbor hopping only and with a box distribution of on-site energies of width W. For $W \neq 0$ these data are averages over 50 different realizations of disorder, and the final results are found using a histogram method with a bin width of $\delta = 0.1t$. The chosen values of W correspond to below, at, and above the critical disorder $W_c/t = 14.5$.

$$\Delta_3(K) = \left\langle \frac{1}{K} \min_{A,B} \int_x^{x+K} [N(\varepsilon) - A\varepsilon - B]^2 d\varepsilon \right\rangle_x \qquad (3)$$

where $N(\varepsilon)$ is the integrated density of states, and $\langle \ldots \rangle_x$ denotes an average over different parts of the energy spectrum. At the critical value of disorder this statistic will be invariant with system size, whereas above and below this value of W it will flow to so-called Poissonian and Gaussian orthogonal ensemble (GOE) limits corresponding to localized and extended states, respectively. The utility of this statistic can be noted in its success in identifying W_c/t for a variety of models and lattices—an example for this model of disorder for the isotropic $3d$ simple cubic lattice is discussed in Ref. 21 and for the anisotropic $3d$ simple cubic lattice in Refs. 29 and 30. Many details of the algorithm that is employed calculating this statistic, including the application of this methodology to the study of other problems, are given in Refs. 27 and 28.

We performed these calculations for system sizes up to 16 000 sites when the eigenvectors were required and for sizes up to 43 904 sites when only the eigenvalues were evaluated. In a small number of instances we evaluated the eigenvectors for system sizes up to 27 648 and found that our predictions based on smaller lattices did not change when these results were included.

IV. NUMERICAL RESULTS

We constructed the complete Anderson-disordered Hamiltonians for CSTL's with different realizations of box disorder (random diagonal elements between $-W/2$ and $W/2$), using periodic boundary conditions, and these have been diagonalized. In Fig. 1 we show some representative density of states (DOS), including the same quantity for an ordered lattice.

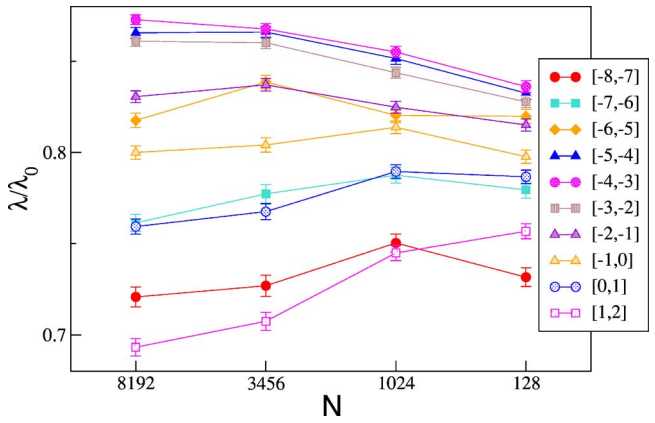

FIG. 2. (Color online) The variation of the relative localization length for lattice sizes from 128 to 8192 sites of CSTL's with periodic boundary conditions, as a function of different energy ranges, for $W/t = 13.5$.

The data for disordered systems correspond to a system size of 21 296 sites averaged over 50 realizations of disorder. The disorder strengths correspond to below, equal to, and above the critical disorder (discussed below). The evolution of the DOS from the ordered to the disordered systems shows that the zero of the DOS at an energy of $-2t$ (for the ordered lattice) becomes a small dip at much lower energies, but this dip is not associated with the lower mobility edge to be concrete, at the critical disorder this dip is present but the upper and lower mobility edges have merged (as we show below, they merge at an energy around $-4t$). At high disorder, as expected, the DOS is approximately symmetric around an energy of zero. Last, the band edges are qualitatively similar to those predicted in analytical calculations.[24]

Clearly, when the disorder strength is not large (relative to W_c) the density of states is not symmetric about some "middle" energy, and to clarify previous comments we note that this necessitates that a search for the mobility edges must include a broadband of energies in the spectrum. In fact, as we discuss below, we find that the mobility edges merge at an energy around $-4t$, which is not that close to the middle of the band for $W \sim W_c$ (as seen in the figure, this middle is around $-0.5t$). Only in the very large W/t limit does the DOS become approximately symmetric about zero energy.

The relative localization length λ/λ_0 was calculated for system sizes of $N = 128$ to 16 000 sites, and these results were averaged over sufficient realizations to obtain converged statistics. Typically, this required an average over a total of roughly 5000 eigenstates in an energy range of $\Delta E = 1.0t$ for any of these system. We found that our numerics displayed the desired self-averaging over complexions for the larger lattices.

A plot displaying typical data is shown in Fig. 2 for a system sizes up of 8192 sites—this corresponds to a W/t ratio that is roughly 7% below the critical disorder (see below). For energy bins that do not include any extended states, the relative localization decreases quite strongly as N is increased, as is seen above ($E \in [1,2]$) and below ($E \in [-8, -7]$) the extended-state energy range—these are states in the

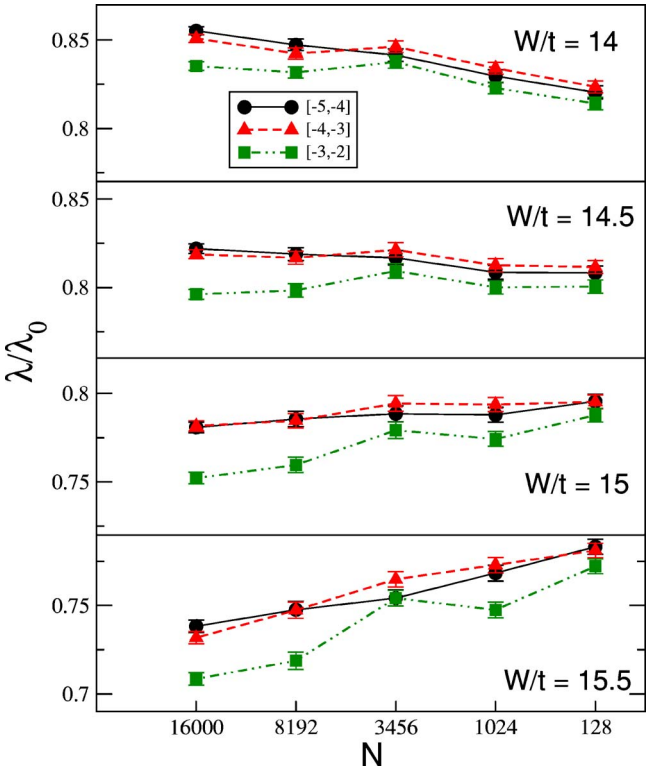

FIG. 3. (Color online) Variation of the relative localization length for systems from N=128 to 16 000 sites for W/t= 14, 14.5, 15, and 15.5. Note that the vertical scales are identical, thus demonstrating the increased (negative) slope of the relative localization length as N and W/t are increased.

upper- and lower-mobility tails, respectively. As one approaches the extended-state region from above ($E \in [0,1]$) and below ($E \in [-7,-6]$) the decrease of the relative localization length with system size is less pronounced and the overall magnitude of this quantity is increased; these states are also in the mobility tails, but are closer in energies to the mobility edges. However, for states inside the energy range $E \in [-5,-2]$ we see unambiguously that the relative localization length grows as the system size is increased and these states correspond to extended states. In the intervening energy ranges ($E \in [-2,0]$ and $[-6,-5]$), the lattice sizes shown are too small to clearly identify the extended versus localized nature of the eigenstates.

Based, in part, on these results, we examined lattice sizes up to 16 000 sites in the energy range $E \in [-5,-2]$ with increasing W/t to determine when states in this energy region became localized, and our results are shown in Fig. 3 (note that the vertical scales are identical in the four frames). For all energy ranges one sees a clear progression from extended to localized behavior with increasing W/t, indicated by both the scaling with system size and the overall magnitude of the relative localization length. For $W/t=14$, states in the energy range $E \in [-5,-2]$ are extended, while for $W/t=15.5$ these states are localized. Also, these data are consistent with states in the energy range $E \in [-3,-2]$ being localized for $W/t=15$. This then implies that the mobility edges merge at an energy around $-4t$, and further, these data thus allow us to

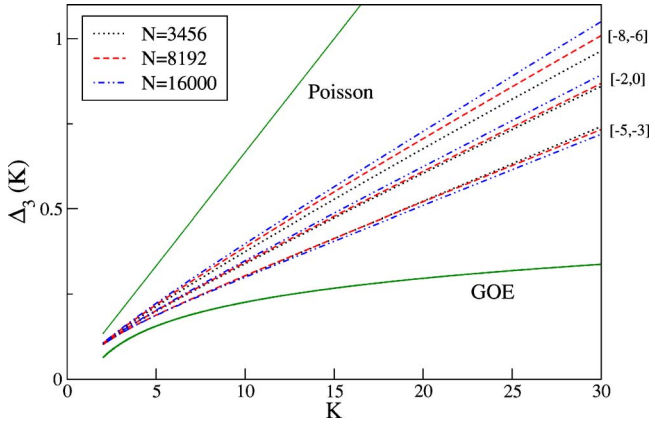

FIG. 4. (Color online) The Dyson-Mehta spectral rigidity Δ_3 plotted for different energy ranges and system sizes, for $W/t=14$. In the range $E \in [-5,-3]$ these data scale towards the GOE statistics (lower curve) or correlated energy levels, whereas for both $E \in [-5,-3]$ and $E \in [-5,-3]$ these data scale towards the uncorrelated result of the Poissonian limit (upper curve). For clarity we only show three system sizes—other sizes obey the scaling inferred from the shown data. The two limiting curves correspond to (uncorrelated) Poissonian statistics and (correlated) Gaussian-orthogonal-ensemble statistics.

identify a clear upper bound of $W_c/t<15.5$. Further, recalling our earlier statements regarding the scale invariance of the spectral rigidity for $W=W_c$, if we also note the approximate independence of system size of the relative localization length for $W/t=14.5$ and 15, we expect that W_c/t will be in this range.

In order to identify the mobility-edge trajectories it is advantageous to first have a reliable value for W_c/t, but from the above-described relative localization length data we cannot be more accurate than $W_c/t \sim 14.5-15$. Instead, we have found that a determination of both the mobility-edge trajectories and the critical disorder may be obtained using the scaling of the Δ_3 "spectral rigidity" of Eq. (3). To be specific, if this quantity scales to the Poissonian limit of uncorrelated energy levels as the size of the system is increased, then the states in that energy range are localized, and if this quantity scales to the GOE limit, the states are extended.[26]

We have studied systems having up to 27 648 sites, which is close to the number of sites in a 30 simple cubic lattice, and have ensured that for all system sizes a sufficient number of realizations are used such that the spectral rigidity was converged for a given W/t and a given system size; sometimes, this required that about 2 000 000 eigenvalues be collected. (For a small number of W/t we have found a smaller number of eigenvalues for system sizes up to 43 904, and these results are consistent with the data that we present below.) For $W/t=14$ example data are shown in Fig. 4. In the energy range of $E \in [-5,-3]$ that was identified through the use of the relative localization length (as corresponding to extended states as the mobility edges approach one another) Δ_3 moves towards GOE statistics, whereas in the $E \in [-8,-6]$ and $[-2,0]$ ranges it moves towards the Poissonian limit. Further, in the energy ranges $E \in [-3,-2]$ and $[-6,-5]$ we find that there is no clear scaling with an in-

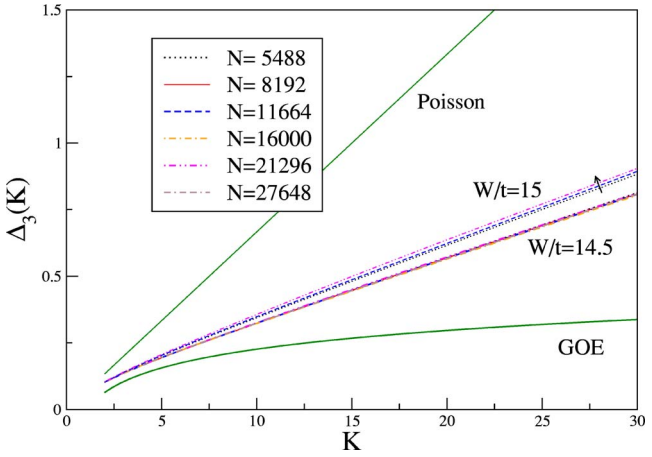

FIG. 5. (Color online) Scale invariance of the spectral rigidity showing that for the values of $W/t=14.5$ and 15, over the energy window $E\in[-5,-3]$, this quantity is independent of system size for $W/t=14.5$ and scales towards the Poissonian uncorrelated limit for $W/t=15$. We note for comparison that these lattice sizes are approximately equivalent to 18, 20, 23, 25, 28, and 30 cubed simple cubic lattices. The Poisson and GOE limits are discussed in a previous caption. The arrow shows the direction that the curves are moving, for $W/t=15$, with increased system sizes (for clarity we only show three system sizes for $W/t=15$).

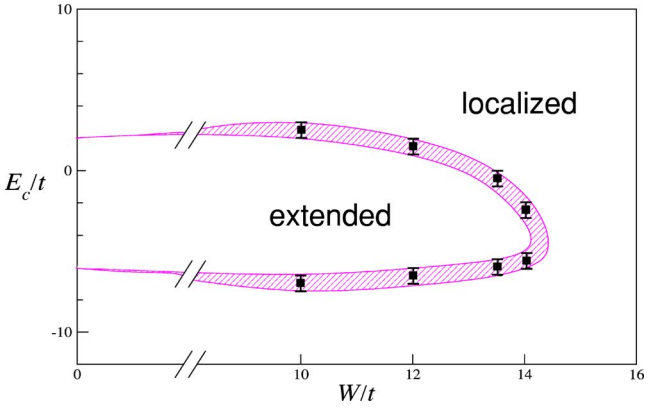

FIG. 6. (Color online) The mobility-edge trajectories (estimates bounded by hatched region) separating localized and extended states on a CSTL for a box distribution of on-site energies of width W, with our data points (solid squares) and error bars interpolated by the boundaries of the hatched region.

crease in system size—that is, the spectral rigidity oscillates with system size in these two energy ranges, indicating the presence of both localized and extended states, and thus one can clearly identify that a mobility edge is to be found in this range.

As mentioned above, we can also use numerical results for the spectral rigidity to determine an accurate value of W_c/t. That is, if we examine all energy ranges around $E\in[-5,-3]$ and find a scaling of Δ_3 to the Poissonian limit for large system sizes, then these states are localized and such values of W_c/t are above the critical disorder strength. Further, we can use the scale invariance of the spectral rigidity to precisely identify W_c/t, and our results are shown in Fig. 5. We find that for $W/t=14.5$ this quantity is independent of system size. We examined a mesh of $\Delta W/t=0.25$ for W/t around 14.5, but found that for precisely $W/t=14.5$ the scale invariance was the most robust—the curves for all system sizes are very nearly coincident and, most importantly, fluctuate in a very small width about an average (as opposed to moving towards the Poissonian or GOE limits). So our final number for the critical disorder of a box distribution of disorder in an Anderson model for CSTL's is $W_c/t=14.5\pm0.25$. For $W/t=15$ this figure shows that the states in this energy range are scaling towards the uncorrelated limit, thus confirming that such disorder is in excess of the critical disorder.

Using such a combined relative localization length and spectral rigidity approach, we have identified the mobility edges for a variety of W/t, and our estimates for these energies as a function of disorder are shown in Fig. 6. As discussed previously, it is interesting to note that the energy at which the mobility edges merge at W_c/t is not in the middle of the density of states (also see Fig. 1); further, unlike the simple cubic lattice, our data for the mobility edges show that they do not rapidly coalesce as W_c/t is approached from below. Instead, the upper mobility edge approaches the energy at which the two edges merge much more gradually—for comparison, see Fig. 1 of Ref. 31.

One further comparison of these results to previously published data for three-dimensional simple cubic lattices involves the magnitude of W_c/t—note the well-accepted result for the critical value of W_c/t for the simple cubic lattice: viz., 16.5.[31–36] At this time we do not have a reliable explanation for the decreased value of W_c/t of the CSTL, something that can only be realized with detailed analytical work. However, if one follows the logic that W_c should be close to the noninteracting bandwidth, which is $12t$ for the simple cubic lattice and $8t$ for the CSTL, and thus reexpresses W_c in units of the bandwidth (which here we label by B), then $W_c/B\sim1.4$ for the simple cubic lattice and $W_c/B\sim1.8$ for the CSTL, and thus one sees that in these scaled units the critical disorder is in fact larger in CSTL's than in a simple cubic lattice. One can speculate that the increase of W_c/B follows from the various near neighbors in these two lattices—we have listed the near neighbors up to the tenth "shell" in Table I. From this one sees that in the third and fourth shells the CSTL has many more neighboring sites on which to form delocalized states than does the simple cubic lattice, so perhaps this difference between these lattices is partly responsible for the large increase of W_c/B in the CSTL in comparison to the simple cubic lattice.

V. APPLICATION TO $LiTi_2O_4$

We have presented comprehensive numerical results for a box distribution of random on-site energies for CSTL having near-neighbor hopping only. We have used the relative localization length and spectral rigidity to identify the mobility-edge trajectories as a function of the width of the box distribution and have determined that $W_c/t\sim14.5$ is the critical disorder at which the upper and lower mobility edges merge. These results aid us in understanding results presented below for disordered $LiTi_2O_4$.[37]

TABLE I. A comparison of the number of nearest neighbors (NN) for simple cubic and CSTL's.

Near Neighbors	Simple cubic lattice	CST lattice
First	6	6
Second	12	12
Third	8	12
Fourth	6	12
Fifth	24	24
Sixth	24	6
Seventh	12	18
Eighth	30	12
Ninth	24	24
Tenth	24	36

As was discussed in the Introduction, our work on this problem was motivated by our interest in the metal-to-insulator transition undergone by $Li_{1+x}T_{2-x-y}Al_yO_4$. One way to go beyond the quantum-site percolation calculations discussed in Ref. 10 is to include the change of the on-site energies due to the impurity potentials, and we have determined the distribution of on-site energies produced by these impurity potentials (using different models of screening). A detailed analysis of the resulting distributions, independent of the model of screening used, indicated that almost all of these energies were between approximately $\pm t$, which, if represented by an Anderson model with a box distribution of on-site energies, would correspond to $W/t=2$, well below $W_c/t=14.5$ for CSTL.

To determine this estimate, a particular complexion of disorder is considered in which the Al ions are placed randomly on the octahedral sites of the spinel structure (the Ti sites of the ordered crystal) according to y, which determines the concentration of Al impurities, and then the screened Coulombic potential from all Al sites is summed up for each of the (nondisordered) Ti sites—these energies thus approximate the (relative) on-site energies of the Ti sites in the disordered lattice. This procedure is repeated for many different realizations of disorder. An example plot of such a distribution on-site energies is given in Fig. 7 for the case of Lindhard screening, which is introduced in the usual manner;[38] very similar distributions are found for a Thomas-Fermi model of screening. Thus, we do not expect the inclusion of this "additional disorder" to produce a substantial change of the results found before,[10] for which the only disorder effects that were included arose from quantum-site percolation.

Indeed, that is what we concluded when we repeated the calculations described in Ref. 10 but now adding in the varying on-site energies generated by the Al impurity potentials—our results for $LiAl_yTi_{2-y}O_4$ when a Lindhard model of screening is used are shown in Fig. 8. We find that the critical value of Al doping that leads to a metal-to-insulator transition is reduced from $y_c \approx 0.82$ for a model that includes quantum-site percolation only to $y_c \approx 0.78$ when the effects of impurity potentials are also included. That is, the role played by the impurity potential disorder is minimal—the lower-mobility-edge energy, for a given disorder, is increased only moderately in a model that includes the effects of the Al impurity ion potentials.

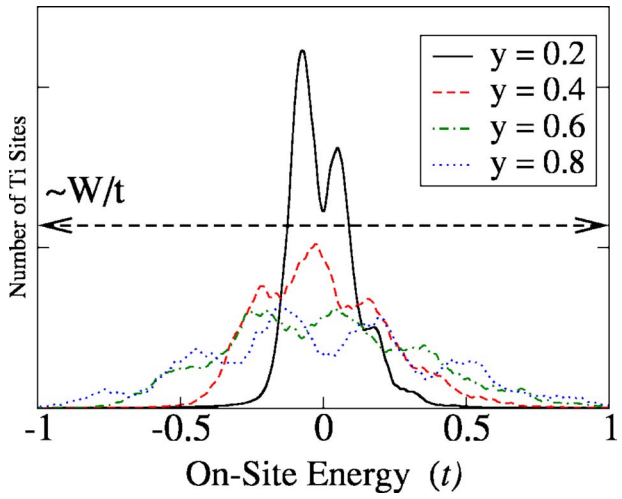

FIG. 7. (Color online) The distribution of the on-site energies of the Ti sites in a disordered lattice as a function of Al concentration y. These energies are found in a Lindhard model of screening of the impurity potentials.

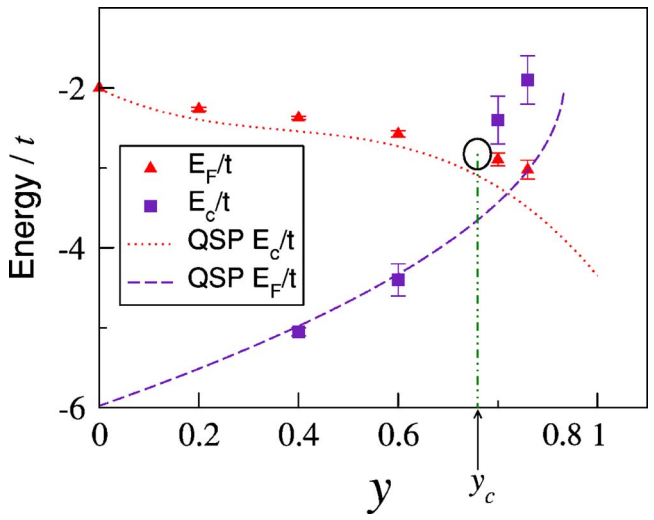

FIG. 8. (Color online) The numerically determined phase diagram for the identification of the critical doping concentrations of the metal-to-insulator transition in $LiAl_yTi_{2-y}O_4$ after including the on-site energies from the screened Coulomb potentials of the doping Al^{3+} ions; the Lindhard approximation is used for screening potentials. The data shown are the Fermi energies (E_F) and mobility edges (E_c) as a function of doping for $LiAl_yTi_{2-y}O_4$ system. Dashed lines (dotted and dashed) are estimates of the Fermi energies and the mobility edges from our previous calculations of the quantum-site percolation (QSP) model only—see Ref. 10. The open black circle is the new estimate of the Al concentration at which one would find a metal-to-insulator transition, in a model that includes the effects of both quantum-site percolation and the inhomogeneous distribution of on-site energies caused by the Al impurity potential.

VI. CONCLUSIONS

We have determined the mobility-edge trajectories and the critical disorder for corner-sharing tetrahedral lattices, lattices that are common in studies of fully frustrated magnetic systems, as well as the sublattice of octahedral sites of a normal spinel structure. We have examined the metal-to-insulator transition of $LiAl_yTi_{2-y}O_4$ and determined that a quantum-site percolation model plus Anderson-like on-site disorder produced by impurity potentials leads to a critical doping of $y_c \approx 0.78$, only 5% less than one estimates if Anderson disorder is ignored and only quantum-site percolation is studied. Since $y_c \approx 0.33$ is the experimental value,[37] indirectly this result supports the hypothesis that something beyond one-electron physics is required to explain this transition—e.g., strong electronic correlations. This possibility will be addressed in a future publication.[11]

ACKNOWLEDGMENTS

We thank George Sawatzky, Bill Atkinson, and Gene Golub for helpful comments and Pakwo Leung for making available some of his computing resources. This work was supported in part by the NSERC of Canada and the Ontario Graduate Scholarship in Science and Technology program.

*Present address: Department of Physics, University of Windsor, Windsor, ON N9B 3P4, Canada.

†Present address: NINT and the Department of Engineering Physics, University of Alberta, Edmonton, AB T6G 2V4, Canada.

[1] See, e.g., the conference proceedings in Can. J. Phys. **79**, 11–12 (2001).

[2] P. W. Anderson, Phys. Rev. **102**, 1492 (1958).

[3] S. T. Bramwell and M. J. P. Gingras, Science **294**, 1495 (2001).

[4] H. Aoki, J. Phys.: Condens. Matter **16**, V1 (2004).

[5] T. F. W. Barth and E. Posnhak, Z. Kristallogr. **82**, 325 (1932).

[6] J. B. Goodenough, Phys. Rev. **117**, 1442 (1960).

[7] S. Kondo, D. C. Johnston, C. A. Swenson, F. Borsa, A. V. Mahajan, L. L. Miller, T. Gu, A. I. Goldman, M. B. Maple, D. A. Gajewski, E. J. Freeman, N. R. Dilley, R. P. Dickey, J. Merrin, K. Kojima, G. M. Luke, Y. J. Uemura, O. Chmaissem, and J. D. Jorgensen, Phys. Rev. Lett. **78**, 3729 (1997).

[8] D. C. Johnston, J. Low Temp. Phys. **25**, 145 (1976).

[9] K. A. Müller, in *Proceedings of the 10th Anniversary HTS Workshop on Physics, Materials and Applications*, edited by B. Batlogg *et al.* (World Scientific, Singapore, 1996), p. 3.

[10] F. Fazileh, R. J. Gooding, and D. C. Johnston, Phys. Rev. B **69**, 104503 (2004).

[11] F. Fazileh, R. J. Gooding, W. A. Atkinson, and D. C. Johnston, Phys. Rev. Lett. (to be published).

[12] F. Fazileh, Ph.D. thesis, Queen's University, 2005.

[13] S. Fujimoto, Phys. Rev. B **64**, 085102 (2001).

[14] S. Fujimoto, Phys. Rev. B **65**, 155108 (2002).

[15] S. Fujimoto, Phys. Rev. Lett. **89**, 226402 (2002).

[16] S. Fujimoto, Phys. Rev. B **67**, 235102 (2003).

[17] C. Chen, Phys. Lett. A **303**, 81 (2002).

[18] Y. Imai and N. Kawakami, Phys. Rev. B **65**, 233103 (2002).

[19] M. Schreiber, F. Milde, and R. A. Römer, Comput. Phys. Commun. **121–122**, 517 (1999).

[20] B. Bulka, M. Schreiber, and B. Kramer, Z. Phys. B: Condens. Matter **66**, 21 (1987).

[21] E. Hofstetter and M. Schreiber, Phys. Rev. B **48**, 16979 (1993).

[22] C. M. Soukalis, Q. Li, and G. S. Grest, Phys. Rev. B **45**, 7724 (1992).

[23] D. E. Sigeti, X. Zhang, M. S. Friedrichs, and R. A. Friesner, Phys. Rev. B **44**, 614 (1991).

[24] F. Wegner, Z. Phys. B: Condens. Matter **36**, 209 (1980).

[25] F. Evers and A. D. Mirlin, Phys. Rev. Lett. **84**, 3690 (2000).

[26] We have also completed extensive analysis of this system using the second moment of the inverse participation ratio, and these data further confirm the results presented in this paper.

[27] O. Bohigas and M. J. Giannoni, Ann. Phys. (N.Y.) **89**, 393 (1975).

[28] O. Bohigas and M. J. Giannoni, in *Mathematical and Computational Methods in Nuclear Physics*, edited by J. S. Dehesa *et al.* (Springer-Verlag, Berlin, 1983), p. 1.

[29] F. Milde, R. A. Römer, and M. Schreiber, Phys. Rev. B **55**, 9463 (1997).

[30] F. Milde, R. A. Römer, and M. Schreiber, Phys. Rev. B **61**, 6028 (2000).

[31] A. MacKinnon and B. Kramer, Z. Phys. B: Condens. Matter **53**, 1 (1983).

[32] H. Grussbach and M. Schreiber, Phys. Rev. B **51**, 663 (1995).

[33] K. Slevin and T. Ohtsuki, Phys. Rev. Lett. **78**, 4083 (1997).

[34] I. K. Zharekeshev and B. Kramer, Phys. Rev. Lett. **79**, 717 (1997).

[35] T. Kawarabayashi, T. Ohtsuki, and K. Slevin, Physica B **284–288**, 1549 (2000).

[36] K. Slevin and T. Ohtsuki, Phys. Rev. B **63**, 045108 (2001).

[37] P. M. Lambert, P. P. Edwards, and M. R. Harrison, J. Solid State Chem. **89**, 345 (1990).

[38] N. W. Ashcroft and N. D. Mermin, *Solid State Physics* (Saunders College, Philadelphia, 1976).